Bioorganic & Medicinal Chemistry 22 (2014) 804–812

Contents lists available at ScienceDirect

Bioorganic & Medicinal Chemistry

journal homepage: www.elsevier.com/locate/bmc

Synthesis and biological evaluation of both enantiomers of [^{18}F]flubatine, promising radiotracers with fast kinetics for the imaging of α4β2-nicotinic acetylcholine receptors

René Smits [a], Steffen Fischer [b], Achim Hiller [b], Winnie Deuther-Conrad [b], Barbara Wenzel [b], Marianne Patt [c], Paul Cumming [a], Jörg Steinbach [b], Osama Sabri [c], Peter Brust [b], Alexander Hoepping [a,*]

[a] ABX Advanced Biochemical Compounds GmbH, Heinrich-Glaeser-Strasse 10-14, D-01454 Radeberg, Germany
[b] Helmholtz-Zentrum Dresden-Rossendorf, Research Site Leipzig, Institute of Radiopharmacy, Permoserstrasse-15, D-04318 Leipzig, Germany
[c] Department of Nuclear Medicine, University of Leipzig, Liebigstrasse 18, D-04103 Leipzig, Germany

ARTICLE INFO

Article history:
Received 9 September 2013
Revised 29 November 2013
Accepted 5 December 2013
Available online 12 December 2013

Keywords:
Alzheimers's disease (AD)
Nicotinic acetylcholine receptor (nAChR)
Flubatine
PET
Fluorine-18

ABSTRACT

Both enantiomers of the epibatidine analogue flubatine display high affinity towards the α4β2 nicotinic acetylcholine receptor (nAChR) in vitro, accompanied by negligible interactions with diverse off-target proteins. Extended single dose toxicity studies in rodent indicated a NOEL (No Observed Effect Level) of 6.2 μg/kg for (−)-flubatine and 1.55 μg/kg for (+)-flubatine. We developed syntheses for both flubatine enantiomers and their corresponding precursors for radiolabeling. The newly synthesized trimethylammonium precursors allowed for highly efficient ^{18}F-radiolabelling in radiochemical yields >60% and specific activities >750 GBq/μmol, thus making the radioligands practical for clinical investigation.

1. Introduction

The increasing economic burden on health care systems presented by the burgeoning incidence of Alzheimer's disease (AD) in societies with aging populations raises the urgent need for improved disease-modifying treatments and early diagnostics. In recent years, much emphasis has been placed on the molecular imaging of amyloid plaques, one of the hallmark neuropathological findings of AD. A number of tracers have been developed for positron emission tomography (PET) studies of amyloid accumulation in suspected AD patients,[1,2] which was previously assessable only through histological examination of post mortem tissue. However, evidence emerging from early trials of therapies targeting amyloid deposition have indicated relatively modest clinical benefits,[3] which calls into question the central role which has been attributed to amyloid processing in the pathogenesis of AD, and highlights the need for more selective neurochemical markers of AD pathology. The nicotinic acetylcholine receptors (nAChRs) in brain participate importantly in aspects of cognition in animals and humans,[4] and have emerged as important targets for the amelioration of AD symptoms. The predominant nAChR in brain is the α4β2-subtype, which constitutes about 90% of the total, and is most abundant in thalamus, hippocampus and frontal cortex.[5,6] Post mortem studies of patients dying with AD have revealed a loss of α4β2 binding sites throughout cerebral cortex,[7] to an extent correlating with the local amyloid concentration.[8] However, the dynamics of cholinergic changes during disease progression is difficult to establish on the basis of post mortem studies.

A number of ligands have been developed for molecular imaging of α4β2 nAChRs in living brain. Studies with (S)(−)-[^{11}C]-nicotine,[9] [^{123}I]-5-iodo-3-(2(*S*)-azetidinylmethoxy)pyridine ([^{123}I]-5IA)[10] and 2-[^{18}F]Fluoro-3-(2(*S*)-azetidinylmethoxy)pyridine (2-[^{18}F]FA)[11] have shown an association between impaired cognitive function in AD and decreased α4β2 nAChR levels in cerebral cortex. However, due to their low specific binding or excessively slow kinetics, none of these tracers are optimal for the sensitive detection of nAChR changes. Therefore, azetidine derivatives of A85380 and bipyridyl-derivatives of epibatidine have been developed recently to overcome these drawbacks.[12,13]

Abbreviations: AD, Alzheimers's disease; nAChR, nicotinic acetylcholine receptor; 2-[^{18}F]FA, 2-[^{18}F]fluoro-3-(2(*S*)-azetidinylmethoxy)pyridine; PET, positron emission tomography; 5-[^{123}I]IA, 5-[^{123}I]-5-iodo-3-(2(*S*)-azetidinylmethoxy)pyridine; HPLC, high performance liquid chromatography; p.s., particle size; ROI, regions of interest; PSL/mm^2, photostimulated luminescence per area.

* Corresponding author. Tel.: +49 3528 4041164; fax: +49 3528 404160.
E-mail address: hoepping@abx.de (A. Hoepping).

0968-0896/$ - see front matter © 2013 Elsevier Ltd. All rights reserved.
http://dx.doi.org/10.1016/j.bmc.2013.12.011

Another approach was adopted by our group. C1-homologation of one C_2-bridge of the epibatidine azabicycle leads to homoepibatidines. Initial findings with the novel homoepibatidine derivative [^{18}F]flubatine **1** (Fig. 1), which was formerly known as [^{18}F]NCFHEB or [^{18}F]norchloro-fluoro-homoepibatidine, revealed similar high affinity at the α4β2 receptor for both enantiomers in vitro,[14] and favourable binding kinetics in mice,[15] pigs[16] and rhesus monkeys.[17] Dynamic PET recordings for quantitation lasted less than two hours, in contrast to the very prolonged recordings required for 2-[^{18}F]FA. These very promising results prompted us to move our program to the clinical stage. A requirement was the development of a new precursor to enable a robust and reliable radiosynthesis as well as the redevelopment of the radiochemistry to allow for an automated radiosynthesis under GMP-conditions.

In our first development of (−)-[^{18}F]flubatine, (−)-[^{18}F]**1** and (+)-[^{18}F]flubatine, (+)-[^{18}F]**1**, the radiosynthesis started from racemic bromo precursor *rac*-**2**, resulting in low radiochemical yield.[18] To improve the outcome of the tracer synthesis, we proposed to develop a precursor carrying a more reactive leaving group and a protecting group that can be cleaved under mild conditions. Furthermore, we sought to synthesize an enantiomerically pure precursor to avoid the requirement for time-consuming chiral HPLC separation of the labeled enantiomers. We now present the synthesis of the Boc-protected, optically pure precursors (−)-**3** and (+)-**3**, both carrying the trimethylammonium leaving group that enables a highly efficient radiolabeling.

2. Results and discussion

2.1. Chemistry

The synthesis of the tropene (8-azabicyclo[3.2.1]octane) framework of the bromo precursor *rac*-**2** uses commercially available *exo*-6-hydroxytropinone as the starting material.[19,20] We decided to synthesize the azabicyclic scaffold via [4+3] cycloaddition, thereby avoiding the use of expensive starting materials and enabling access to multigram quantities of the desired compounds.

The synthetic pathway for the synthesis of the racemic flubatine standard *rac*-**1** is shown in Scheme 1. After [4+3] cycloaddition between the readily available compounds 1,1,3,3-tetrabromopropanone **5**[21] and Cbz-protected pyrrole **4**,[22] the two remaining bromo substituents were removed by reduction with zinc-copper couple.[23,24] Cbz was chosen as the nitrogen protecting group since it can be easily replaced by the desired Boc moiety. Direct introduction of the Boc protecting group using N-Boc-pyrrole as reactant for the [4+3] cycloaddition proved to be ineffective due to poor yields.[25]

The palladium-catalyzed Heck-type hydroarylation[26,27] served to couple 2-fluoro-5-iodopyridine to *meso*-**7**. Although some asymmetric approaches using chiral ligands for the arylation of bicyclic[28,29] or azabicyclic[30] alkenes have been published, the obtained enantiomeric excesses were too low to circumvent separation of enantiomers. Initially, we applied the conditions that were used by Regan et al. for the synthesis of epibatidine.[31] After heating the coupling partners at 80 °C for 22 h in the presence of 8 mol% $(PPh_3)_2Pd(OAc)_2$, piperidine and formic acid, the product *rac*-**8** could be isolated in only 21% yield as an 8:1 mixture of *exo*- and *endo*-isomers. By substituting the palladium catalyst for *trans*-bis(acetato)bis[*o*-(di-*o*-tolylphosphino)benzyl]dipalladium(II)[32] and the base for triethylamine, the yield was increased to 86% after 3.5 h. Moreover, the desired *exo*-product was formed exclusively.

Deoxygenation of the keto-function could be accomplished by applying a modified three-step protocol developed by Kim et al.[33] Thus, the ketone *rac*-**8** was reduced with sodium borohydride. The corresponding diastereomeric alcohols *dia*-**9** were reacted with thiocarbonyl diimidazole to give imidazole thiocarbamate *dia*-**10**, that was deoxygenated under Barton–McCombie conditions to yield *rac*-**11**. Similar yields were obtained when the deoxygenation sequence was performed prior to the hydroarylation reaction, starting from *meso*-**7**. Finally, the Cbz protecting group was cleaved by transfer hydrogenation using cyclohexene as the hydrogen source to give racemic flubatine *rac*-**1**.

Resolution of racemic, azabicyclic ketones via aminals derived from (*R*,*R*)-1,2-diphenylethylenediamine has been applied during a formal epibatidine synthesis.[34] Since separation of different diastereomeric aminals of *rac*-**8** was not feasible by chromatography, chiral HPLC served for the separation of flubatine enantiomers *rac*-**1**. Gram quantities of each enantiomer could be isolated with >99% *ee* using a semipreparative Daicel CHIRALPAK IA column (Scheme 2). The absolute stereochemistry was determined by X-ray crystallography of the (−)-flubatine-(−)-tartrate salt and the (+)-flubatine-(+)-tartrate salt (Fig. 2, see Supporting information for selected data) and was assigned to be (1*R*,5*S*,6*S*) for (−)-**1**.

The synthetic route employed to prepare the enantiomerically pure (−)-flubatine precursor (−)-**3** is outlined in Scheme 3. After nucleophilic aromatic substitution of fluorine in (−)-**1** with dimetylamine, the secondary amino-function was Boc-protected under standard conditions. In the last step of the precursor synthesis, the dimethylaminopyridine **13** had to be methylated to give the corresponding trimethylammonium derivative (−)-**3**. Initial experiments using methyl trifluoromethanesulfonate as the alkylating agent gave considerable amounts of two by-products that could not be separated from the desired product (−)-**3**. The formation of these by-products was minimized by quaternization using methyl iodide.[35] After crystallization, the (−)-flubatine precursor (−)-**3** was isolated in high purity and 70% yield. The overall yield was 5% after 11 steps, starting from Cbz-protected pyrrole **4**. The (+)-flubatine precursor was synthesized in an analogous way from (+)-**1**.

2.2. Radiochemical synthesis of (−)- and (+)-[^{18}F]1

The radiosynthesis of (−)-[^{18}F]**1** was achieved by a two-step procedure entailing first the no-carrier-added nucleophilic radiofluorination of trimethylammonium precursor (−)-**3** and subsequent cleavage of the protecting group (Scheme 4). Reaction of (−)-**3** with K[^{18}F]F-K_{222}-carbonate complex in acetonitrile at 82 °C for 20 min gave the best results, providing (−)-[^{18}F]**14** in 80–95% (n = 40) labeling yield. After deprotection with 1 M HCl at 90 °C for 8 min, (−)-[^{18}F]**1** was separated by semipreparative reverse phase HPLC and solid phase extraction. The overall decay-corrected radiochemical yield was 60 ± 5% (n = 25) and the

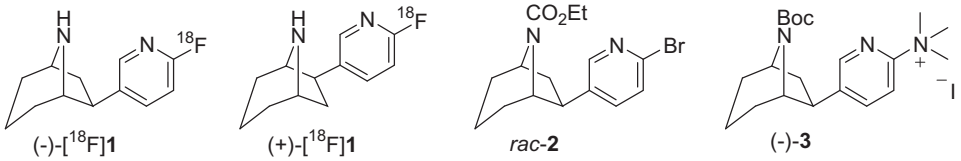

Figure 1. Chemical structures of (−)- and (+)-[^{18}F]flubatine ((−)-[^{18}F]**1** and (+)-[^{18}F]**1**), bromo precursor *rac*-**2** and trimethylammonium precursor (−)-**3**.

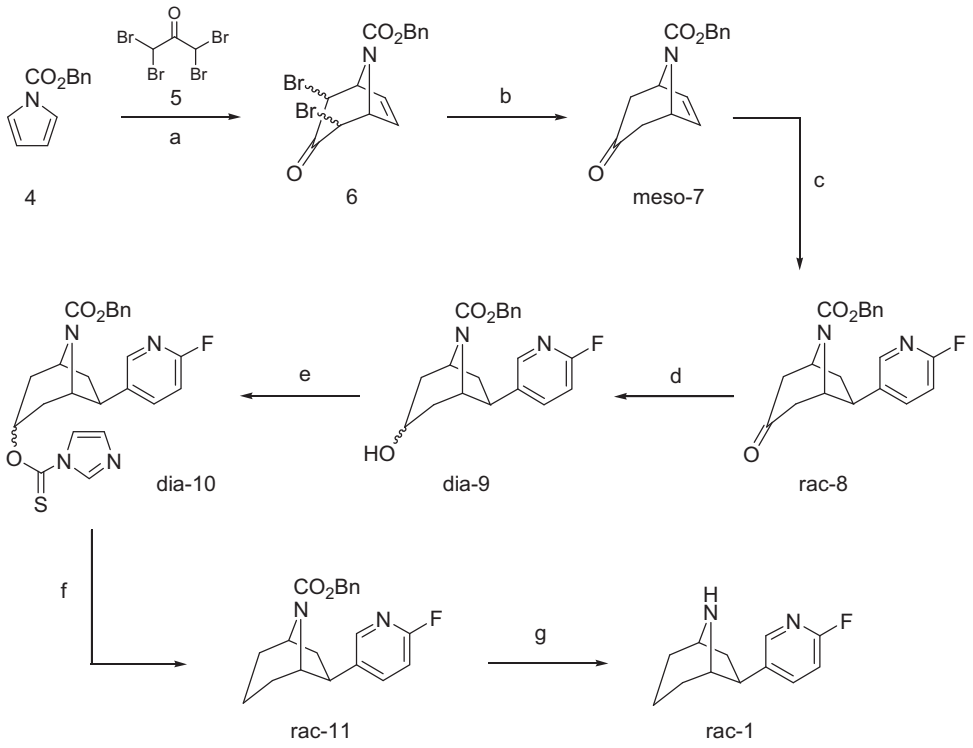

Scheme 1. Synthesis of racemic flubatine *rac*-**1**. Reagents and conditions: (a) diethylzinc, toluene, −12 °C–rt; (b) zinc–copper couple, NH_4Cl, MeOH, rt, 45% (over two steps); (c) 2-fluoro-5-iodopyridine, *trans*-bis(acetato)bis[*o*-(di-*o*-tolylphosphino)benzyl]dipalladium(II), Et_3N, HCO_2H, DMF, 70 °C, 86%; (d) $NaBH_4$, MeOH, 0 °C, 94%; (e) *S*-CDI, toluene, reflux, 93%; (f) Bu_3SnH, AIBN, toluene, reflux, 70%; (g) Pd/C, cyclohexene, EtOH, reflux, 81%.

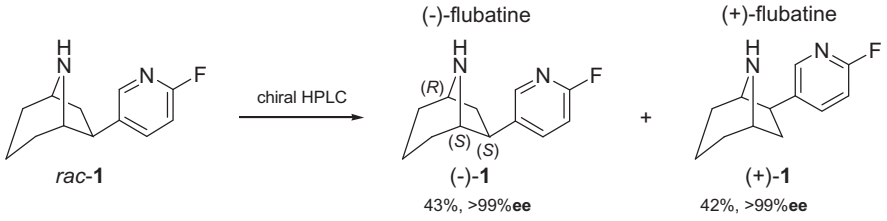

Scheme 2. Resolution of flubatine enantiomers by chiral HPLC.

radiochemical purity >99% after 120 min at the end of radionuclide production. No residual precursor (−)-**3** or intermediate (−)-[^{18}F]**14** was detected in formulated (−)-[^{18}F]**1** by analytical HPLC. Starting from 0.5 GBq [^{18}F]F^-, a specific radioactivity of 350 GBq/μmol was obtained at the end of radiosynthesis. A specific activity of more than 750 GBq/μmol, sufficient for human application was achieved with starting activities between 5 and 45 GBq. (+)-[^{18}F]**1** was synthesized in an analogous way from (+)-**3**. A detailed optimisation study for the radiosynthesis of (−)-[^{18}F]**1** and the fully automated radiosynthesis under GMP conditions was recently published.[36,37]

2.3. Receptor profile and toxicology

High affinity towards human α4β2 nAChR and specificity versus human α3β4 nAChR and human α7 nAChR, determined in vitro by radioligand displacement studies, were already reported for (−)-**1** and (+)-**1**.[14] In order to further characterize their pharmacological selectivity, off-target screening of (−)-**1** and (+)-**1** against 45 other receptors, ion channels and enzymes (listed in detail in the Section 4) was performed by primary and secondary screening binding assays (Eurofins Panlabs). The K_i values obtained for different nAChR subtypes within this new study confirm the previously determined high specificity of binding of (−)-**1** and (+)-**1** towards α4β2 nAChR versus other nAChR subtypes (rat α4β2: 0.13 and 0.22 nM; human α3β4: 2.03 and 3.99 nM; rat α7: 5.75 and 4.43 μM, respectively). Furthermore, besides a 61% inhibition of the binding of [^{3}H]pyrilamine to human H_1 receptors, neither (−)-**1** nor (+)-**1** interacted significantly (⩾50% inhibition) with any other of the off-target proteins investigated at a concentration of 10 μM. Although no direct comparative studies were performed using other thoroughly investigated ligands of α4β2 nAChR such as A-85380, sazetidine, or nifene, the results of the affinity, specificity, and selectivity investigations indicate the suitability of (−)-**1** and (+)-**1** for molecular imaging of α4β2 nAChR.

Both compounds were assessed for their toxicological effects according to the relevant international guidelines. In extended single dose toxicity studies (−)-**1** and (+)-**1** were administered intravenously to groups of male and female Wistar rats at low, medium, and high doses. For (−)-**1** doses of 6.2, 24.8, and 124 μg/kg (Harlan Laboratories, Itingen, Switzerland) and for (+)-**1** doses of 1.55, 12.4, and 21.7 μg/kg (BSL BIOSERVICE Scientific Laboratories GmbH, Planegg, Germany) were administered. One half of the animals were killed on day two pi, the remaining animals were killed on day 14. Acute manifestation of clinical signs such as tachypnea, labored breathing, and cyanosis were observed in medium and high

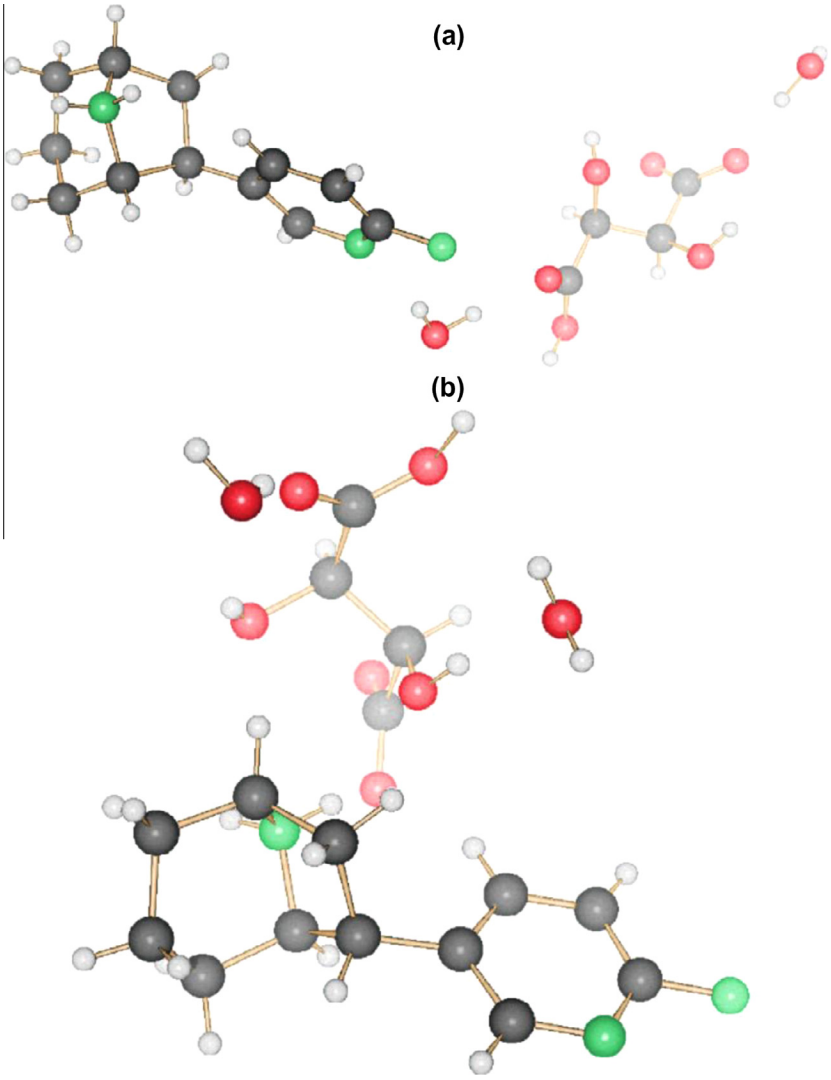

Figure 2. X-ray structure of (−)-flubatine-(−)-tartrate (a) and (+)-flubatine-(+)-tartrate (b).

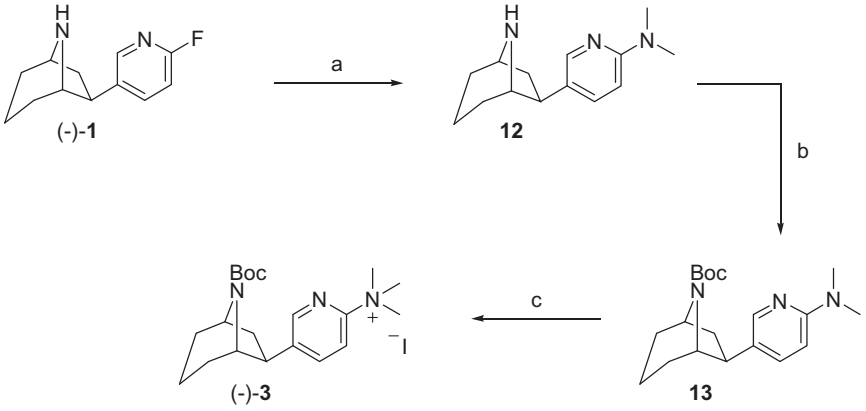

Scheme 3. Synthesis of the enantiomerically pure (−)-flubatine precursor (−)-**3**. Reagents and conditions: (a) dimethylamine (5.6 M in EtOH), autoclave, 100 °C, 86%; (b) Boc_2O, Et_3N, THF, 95%; (c) MeI, K_2CO_3, MeOH, 70%.

dose groups, whereas no symptoms were detected in low dose groups. Histopathology in the 14 day survival group revealed no macroscopic or microscopic findings. On the basis of the results of these studies, a NOEL (No Observed Effect Level) of 6.2 μg/kg for (−)-**1** and 1.55 μg/kg for (+)-**1**, respectively was calculated for application in humans, based upon conventional scaling of dose to body weight. The NOEL for the more toxic enantiomer (+)-**1** would require a specific activity exceeding 700 GBq/μmol in order to maintain a 1000-fold safety margin for the application of the compound in clinical studies.

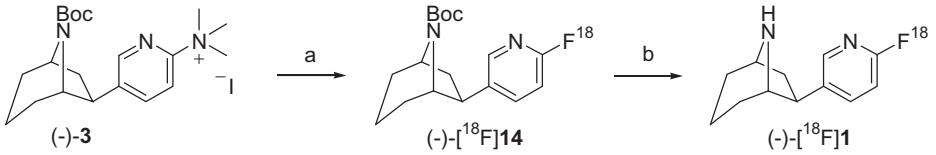

Scheme 4. Radiosynthesis of (−)-[^{18}F]**1**. Conditions: (a) K[^{18}F]F, K_{222}, K_2CO_3, MeCN, 82 °C; (b) 1 M HCl, 90 °C; then 1 M NaOH.

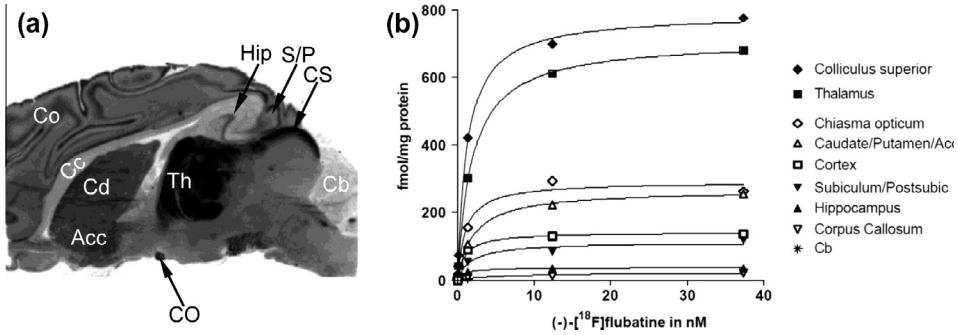

Figure 3. Binding of (−)-[^{18}F]**1** on sagittal brain slices (20 μm) from pig in vitro. (a): representative in vitro autoradiograph of the distribution of 4 nM (−)-[^{18}F]**1**. (b): Representative in vitro autoradiographic saturation binding analysis for (−)-[^{18}F]**1** in pig brain cryostat sections. Abbreviations: Acc = nucleus accumbens; Cb = cerebellum; Cc = corpus callosum; Cd = nucleus caudatus; Co = cortex; CO = chiasma opticus; CS = colliculus superior; Hip = hippocampus; Th = thalamus; S/P = subiculum/postsubiculum.

2.4. Autoradiography (pig)

Having the radiotracers (−)-[^{18}F]**1** and (+)-[^{18}F]**1** available, we performed further investigations to estimate the binding parameters of the two tracers directly. Therefore, both the anatomic distribution and the binding parameters of the binding of (−)-[^{18}F]**1** and (+)-[^{18}F]**1** were assessed by autoradiography in pig brain cryostat sections in vitro. Examples of the binding pattern of (−)-[^{18}F]**1** at 4 nM as well as of a saturation analysis of the binding of (−)-[^{18}F]**1** are shown in Figure 3.

The pattern of distribution of (−)-[^{18}F]**1** and (+)-[^{18}F]**1** in sagittal slices of whole hemispheres of the pig brain matches closely with the distribution of binding sites detected by 2-[^{18}F]FA in porcine brain[38] as well as by further α4β2 nAChR specific radiotracers in other species.[39–41] However, few regions known to express α4β2 nAChR in high density were recently detected by autoradiographic studies in rat brain using [^{125}I]AT-1012, a novel but still incompletely characterised α3β4* nAChR radioligand. Since with habenula and nucleus interpeduncularis two of these regions were also labelled by (−)-[^{18}F]**1** and (+)-[^{18}F]**1** in our pig brain studies, the actual relevance of the nanomolar affinites of (−)-[^{18}F]**1** and (+)-[^{18}F]**1** towards α3β4 nAChR for interpretation of imaging data remains to be elucidated. However, even assuming that α3β4 nAChR and α4β2 nAChR are comparably expressed, the ten-fold lower affinity of (−)-[^{18}F]**1** and (+)-[^{18}F]**1** towards the former subtype would contribute to only a small proportion of the specific signal obtained. Thus, despite we were so far not able to assess the expression of either α4β2 nAChR or α3β4* nAChR protein in pig brain by immunodetection due to the limited suitability of commercially available antibodies[42] the autoradiographic data support the suitability of (−)-[^{18}F]**1** and (+)-[^{18}F]**1** for molecular imaging of the α4β2 nAChR subtype in the brain. The binding of (−)-[^{18}F]**1** and (+)-[^{18}F]**1** to each of the investigated brain areas was saturable and apparently monophasic (Fig. 3b), and we estimated K_D values of 1.08 ± 0.06 nM (n = 3) for (−)-[^{18}F]**1** and 1.17 ± 0.6 nM (n = 3) for (+)-[^{18}F]**1** in the thalamus, a region expressing α4β2 nAChR at high density.[43,44]

3. Conclusion

In summary, we have developed a concise synthesis for the preparation of optically pure non-radioactive reference compounds (−)-**1** and (+)-**1**. Boc-protected precursors (−)-**3** and (+)-**3** with trimethylammonium leaving group were accessible from the reference compounds and allowed for highly efficient radiolabeling to afford (−)-[^{18}F]**1** and (+)-[^{18}F]**1**. Preclinical investigation of both radiotracers revealed affinity and selectivity characteristics suitable for specific imaging of α4β2 nAChRs. (−)-[^{18}F]**1**, the enantiomer reported previously to exhibit faster binding kinetics in pig brain, was chosen for initial studies in man. The results of this first human imaging study will be presented in forthcoming publications.

4. Experimental section

4.1. Chemistry

Solvents were purchased from Merck and Fisher Scientific. Chemicals were obtained from Merck, Fisher Scientific, Sigma–Aldrich, C. Roth and Macherey-Nagel. All chemical reagents were of highest commercially available quality and applied without further purification. *Meso*-**7** was synthesized as described in the literature.[24] Thin-layer chromatography (TLC) was performed with Macherey-Nagel precoated plastic sheets with fluorescent indicator UV254 (Polygram® SIL G/UV254). Visualization of the spots was effected by irradiation with an UV lamp (254 and 366 nm). ^{1}H Nuclear magnetic resonance (NMR), ^{13}C NMR and ^{19}F NMR spectra were obtained with Bruker spectrometer (Bruker, AV500). Chemical shifts are reported as δ values. Coupling constants are reported in Hertz. Optical rotations were recorded on a Rudolph Autopol IV Polarimeter and are reported as $[\alpha]_D$ (concentration). Preparative chiral HPLC was performed using a Knauer HPLC consisting of binary pump K-1800 and UV detector K-2501. Chiral HPLC analysis was performed using a Thermo SCIENTIFIC device (Thermo SCIENTIFIC Ultimate 3000 HPLC, Chromeleon) consisting of quaternary pump,

Diode-Array Detector, and autosampler. Electrospray ionisation mass spectra were obtained using a MSQ mass detector (Thermo SCIENTIFIC). Radioluminescence thin layer chromatograms were recorded using a BAS-1800 II system Bioimaging Analyzer (Fuji Film, Japan) and images were evaluated with AIDA 2.31 software (Raytest, Germany). For Solid Phase Extraction (SPE), Sep-Pak® cartridges Plus, OASIS® cartridges (Waters, USA), and Chromafix® cartridges (Macherey-Nagel, Germany) were used. Analytical radio-HPLC was performed using an Agilent device (Agilent 1100 HPLC ChemStation, Agilent Technologies, Santa Clara, CA) consisting of quaternary pump, UV–Vis detector, Diode-Array Detector, NaI(Tl)-scintillation detector (bte, Braunschweig, Germany) for gamma detection, an autosample, and using a Multospher®120 RP18-AQ-5 analytical column (CS Chromatographie Service, Germany) with pre-column (17 × 4.6 mm plus 250 × 4.6 mm, 5 μm particle size (p.s.); eluent: 20% acetonitrile (MeCN) + 31 mM ammonium acetate (NH_4OAc), flow rate 1.0 mL/min), by gradient method A (for the analysis of final radiotracer): 5% MeCN (0–5 min), 5–40% (5–40 min), 40% MeCN + 20 mM NH_4OAc (40–50 min), or gradient method B (quality assurance for non-radioactive impurities): 10% MeCN (0–10 min), 5–90% (10–45 min). The crude ^{18}F-labeled product was purified with a semi-preparative radio-HPLC consisting of a S1021 pump (SYKAM Chromatographie, Germany), UV detector (Well-ChromK-2001, KNAUER, Germany), NaI(Tl)-counter and data acquisition with an automated system (NINA, Nuclear Interface) using a Multospher® 120 RP18 AQ column (150 × 10 mm, 5 μm p.s.; CS Chromatographie Service, Germany); solvent: 25% MeCN/water + 20 mM NH_4OAc; flow rate 1 mL/min. The chiral HPLC system consisted of a Merck-Hitachi LaChrom D-7000 with a L-7100 pump, a Rheodyne injection valve with 20 μl sample loop and a L-7400 UV detector. The polarimetric identification of the enantiomers was performed using a chiral detector (OR-2090, JASCO, Germany). The polarity of signal amplitudes obtained by the chiral detector was verified for each eluent, with (−)-vesamicol as reference compound. Analytical experiments were performed by using Reprosil Chiral-OM (5 μm p.s.), Reprosil Chiral-AM-RP (5 μm p.s.), and Reprosil Chiral-AA (8 μm p.s.) as 250 × 4.6 mm columns and a 150 × 4.6 mm Reprosil Chiral-OM-RP column (5 μm p.s.) from the Dr. Maisch-GmbH, Germany. Furthermore, a ChiralPak® IA column (250 × 4.6 mm, 5 μm p.s.) from Chiral Technologies Europe was tested. Mobile phases were degassed by sonication. Sample solutions were prepared by dissolving of about 1 mg of compounds in 1 mL of an appropriate eluent mixture. The injection volume was 10–20 μL.

4.1.1. (+/−)-*exo*-6-(6-Fluoro-pyridin-3-yl)-3-oxo-8-aza-bicyclo[3.2.1]octane-8-carboxylic acid benzyl ester (*rac*-8)

Triethylamine (1.89 ml, 13.7 mmol, 3.5 equiv) and 2-fluoro-5-iodopyridine (2.17 g, 9.75 mmol, 2.5 equiv) were added to a solution of *meso*-**7** (1.0 g 3.89 mmol) in 6.9 ml of DMF. The solution was placed under argon and *trans*-bis(acetato)bis[*o*-(di-*o*-tolylphosphino)benzyl]-dipalladium(II) (219 mg, 0.234 mmol, 6 mol %) was added. Finally, formic acid (0.39 ml, 10.3 mmol, 2.65 equiv) was added dropwise. The reaction mixture was stirred for 4 h at 70 °C. After cooling to RT the reaction mixture was filtered over celite and washed with ethyl acetate. The filtrate was diluted with ethyl acetate and washed with water. The aqueous phase was extracted twice with ethyl acetate. The combined organic phases were dried over sodium sulfate and the solvent was removed in vacuo. The crude product was purified by column chromatography (ethyl acetate/hexane = 1:2) to afford *rac*-**8** (1.19 g, 86%) as a yellow oil. ^{1}H NMR ($CDCl_3$, 500 MHz) two rotameric forms result in a doubling of some signals: δ = 8.02 (bs, 1H), 7.66–7.49 (m, 1H), 7.46–7.26 (m, 5H), 6.90–6.76 (m, 1H), 5.30–5.13 (m, 2H), 4.88–4.67 (m, 1H), 4.60–4.36 (m, 1H), 3.20 (bs, 1H), 2.91–2.00 (m, 6H).

4.1.2. *exo*-6-(6-Fluoro-pyridin-3-yl)-3-hydroxy-8-aza-bicyclo[3.2.1]octane-8-carboxylic acid benzyl ester (*dia*-9)

Sodium borohydride (677 mg, 17.9 mmol, 1.05 equiv) was added in portions to a stirred solution of *rac*-**8** (6.04 g, 17.05 mmol) in methanol (170 ml) at 0 °C. The reaction mixture was stirred for 20 min at 0 °C before 1 M citric acid was added dropwise till evolution of hydrogen had ceased. The solution was concentrated to a few ml, diluted with 300 ml ethyl acetate and washed with 100 ml saturated sodium bicarbonate solution. The aqueous phase was extracted three times with ethyl acetate. The combined organic phases were dried over sodium sulfate and the solvent was removed in vacuo. The crude product was purified by column chromatography (ethyl acetate/hexane = 2:1 to 3:1) to afford *dia*-**9** (5.75 g, 94%, 1.3:1 mixture of diastereomers) as a yellow oil. The diastereomeric alcohols were separated for characterization. ^{1}H NMR major diastereomer ($CDCl_3$, 500 MHz) two rotameric forms result in a doubling of some signals: δ = 8.02 (bs, 1H), 7.64–7.50 (m, 1H), 7.42–7.26 (m, 5H), 6.85–6.70 (m, 1H), 5.23–5.07 (m, 2H), 4.56–4.42 (m, 1H), 4.26–4.08 (m, 2H), 3.93–3.85 (m, 1H), 2.87–2.76 (m, 1H), 2.29–1.58 (m, 6H). ^{1}H NMR minor diastereomer ($CDCl_3$, 500 MHz) two rotameric forms result in a doubling of some signals: δ = 8.00 (bs, 1H), 7.64–7.49 (m, 1H), 7.43–7.24 (m, 5H), 6.87–6.72 (m, 1H), 5.23–5.08 (m, 2H), 4.62–4.46 (m, 1H), 4.33–4.15 (m, 2H), 3.22–3.11 (m, 1H), 2.24–1.89 (m, 4H), 1.78–1.52 (m, 3H).

4.1.3. *exo*-6-(6-Fluoro-pyridin-3-yl)-3-(imidazole-1-carbothioyloxy)-8-aza-bicyclo[3.2.1]-octane-8-carboxylic acid benzyl ester (*dia*-10)

1,1′-Thiocarbonyldiimidazole (3.7 g, 20.7 mmol, 1.3 equiv) was added to a solution of *dia*-**9** (5.66 g, 15.9 mmol) in 36 ml toluene. The reaction mixture was heated to reflux for two hours. The solvent was removed in vacuo and the crude product was purified by column chromatography (ethyl acetate/hexane = 1:1) to afford *dia*-**10** (6.39 g, 93%, 1.15:1 mixture of inseparable diastereomers) as a white solid. ^{1}H NMR ($CDCl_3$, 500 MHz) two rotameric forms result in a doubling of some signals, mixture of two diastereomers (A/B): δ = 8.39 (s, 1H, A), 8.30 (s, 1H, B), 8.06 (bs, 1H, B), 8.02 (bs, 1H, A), 7.66 (s, 1H, A), 7.59 (s, 1H, B), 7.68–7.50 (m, 1H, A, 1H B), 7.45–7.27 (m, 5H, A, 5H, B), 7.12 (s, 1H, A), 7.04 (s, 1H, B), 6.89–6.73 (m, 1H, A, 1H, B), 6.07–5.96 (m, 1H, B), 5.93–5.86 (m, 1H, A), 5.29–5.11 (m, 2H, A, 2H, B), 4.75–4.52 (m, 1H, A, 1H, B), 4.45–4.19 (m, 1H, A, 1H, B), 3.57–3.48 (m, 1H, A), 3.36–3.26 (m, 1H, B), 2.66 (m, 1H, A), 2.52–2.20 (m, 3H, A, 3H, B), 2.18–1.94 (m, 2H, A, 2H, B), 1.89–1.76 (m, 1H, B).

4.1.4. (+/−)-*exo*-6-(6-Fluoro-pyridine-3-yl)-8-aza-bicyclo[3.2.1]octane-8-carboxylic acid benzyl ester (*rac*-11)

Tributyltin hydride (4.76 ml, 17.7 mmol, 1.4 equiv) and azobisisobutyronitrile (208 mg, 1.26 mmol, 0.1 equiv) were added to a solution of *dia*-**10** (5.47 g, 12.6 mmol) in toluene (68 ml) under argon. The reaction mixture was heated to reflux for 3.5 h. The solvent was removed in vacuo and the crude product was purified by column chromatography (ethyl acetate/hexane = 1:5 to 1:4) to afford *rac*-**11** (3.02 g, 70%) as a white solid. ^{1}H NMR ($CDCl_3$, 500 MHz) two rotameric forms result in a doubling of some signals: δ = 8.01 (bs, 1H), 7.63–7.49 (m, 1H), 7.44–7.27 (m, 5H), 6.85–6.71 (m, 1H), 5.27–5.10 (m, 2H), 4.57–4.42 (m, 1H), 4.25–4.10 (m, 1H), 3.29–3.17 (m, 1H), 2.37–2.24 (m, 1H), 2.00–1.45 (m, 7H).

4.1.5. (+/−)-6-(6-Fluoro-pyridine-3-yl)-8-aza-bicyclo[3.2.1]octane (*rac*-1)

rac-**11** (10.5 g, 30.8 mmol) was stirred in cyclohexene (140 ml) and ethanol (280 ml) until complete dissolution. The solution was placed under argon and 10% palladium on activated carbon (6.55 g,

6.15 mmol, 0.2 equiv) was added carefully. The reaction mixture was heated to reflux for 16 h. After cooling to RT the reaction mixture was filtered over celite. The filtration residue was washed with methanol and the solvent was removed in vacuo. The crude product was purified by column chromatography (methanol/ethyl acetate = 1:3) to afford *rac*-**1** (5.2 g, 81%) as a white solid. ^{1}H NMR ($CDCl_3$, 500 MHz): δ = 8.07 (d, J = 2.2 Hz, 1H), 7.85 (ddd, J = 8.2, 5.6, 2.5 Hz, 1H), 6.84 (dd, J = 8.5, 3.0 Hz, 1H), 3.64–3.70 (m, 1H), 3.31 (s, 1H), 3.15 (dd, J = 9.3, 5.0 Hz, 1H), 2.22 (dd, J = 13.2, 9.3 Hz, 1H), 1.50–1.89 (m, 8H). ^{13}C NMR ($CDCl_3$, 126 MHz): δ = 162.18 (d, J = 236.9 Hz, 4°), 145.55 (d, J = 14.1 Hz, 3°), 141.32 (d, J = 4.5 Hz, 3°), 139.45 (d, J = 7.6 Hz, 4°), 109.19 (d, J = 37.2 Hz, 3°), 62.75 (3°), 55.65 (3°), 44.13 (3°), 39.42 (2°), 33.31 (2°), 32.72 (2°), 17.64 (2°). ^{19}F NMR ($CDCl_3$, 470 MHz): δ = −72.31 to −72.58 (m). MS (ESI+): m/z 206.9 (M^+).

4.1.6. (−)-(1*R*,5*S*,6*S*)-6-(6-Fluoro-pyridine-3-yl)-8-aza-bicyclo[3.2.1]octane ((−)-flubatine, (−)-1) and (+)-(1*S*,5*R*,6*R*)-6-(6-fluoro-pyridine-3-yl)-8-aza-bicyclo[3.2.1]octane ((+)-flubatine, (+)-1)

Chiral resolution was done by semi-preparative chiral HPLC on a 250 × 20 mm, 5 μm p.s., CHIRALPAK® IA column. *rac*-**1** (5.2 g, 25.2 mmol) was dissolved in 42 ml of eluent (MeCN/0.1% diethylamine). The injection volume was 1 ml. Chiral HPLC separation was done under isocratic conditions at a flow rate of 20 ml/min. Detection was performed by means of a UV detector at a wavelength of 280 nm. The retention time of (+)-**1** was approx. 8–13 min, that of (−)-**1**) approx. 19–38 min. Both enantiomers were collected separately, after chiral HPLC the mobile solvent was removed in vacuo. The enantiomeric purity was determined by analytic chiral HPLC on a 250 × 4.6 mm, 5 μm p.s., CHIRALPAK® IA column. 1 mg of the respective enantiomer was dissolved in 1 ml of eluent (methanol/0.1% triethylamine). The injection volume was 10 μl. Isocratic conditions were used at a flow of 1 ml/min. Detection was done at 280 nm. The retention time of (+)-**1** was 11.5 min, that of (−)-**1** 17.5 min. (−)-**1** (2.24 g, 43%, >99% ee, $[\alpha]_D^{20}$ ($CHCl_3$, c = 5 mg/ml) = −30.9°) and (+)-**1** (2.2 g, 42%, >99% ee, $[\alpha]_D^{20}$ ($CHCl_3$, c = 5 mg/ml) = +29.0°), were isolated as white solid, respectively. All other analytical data are identical with those reported for *rac*-1.

4.1.7. (−)-(1*R*,5*S*,6*S*)-[5-(8-Aza-bicyclo[3.2.1]oct-6-yl)-pyridine-2-yl]-dimethylamine (12)

(−)-**1** (1.01 g, 4.9 mmol) was dissolved in dimethylamine solution (49 ml, 5.6 M in ethanol) and transferred to an autoclave. The autoclave was closed and heated to 100 °C for 1 d under stirring. After cooling to RT the solvent was removed in vacuo. The residue was purified by column chromatography (ethyl acetate:methanol:Et_3N = 9:1:0.1) to afford **12** (0.95 g, 4.25 mmol, 86%) as a white solid. ^{1}H NMR ($CDCl_3$, 500 MHz): δ = 8.03 (d, J = 2.4 Hz, 1H), 7.45 (dd, J = 8.8, 2.5, 1H), 6.49 (dd, J = 8.8, 3.0 Hz, 1H), 3.60–3.67 (m, 1H), 3.26 (bs, 1H), 3.07 (dd, J = 9.2, 5.1 Hz, 1H), 3.05 (s, 6H), 2.18 (dd, J = 13.2, 9.2 Hz, 1H), 1.57–1.91 (m, 7H), 1.46–1.54 (m, 1H).

4.1.8. (−)-(1*R*,5*S*,6*S*)-6-(6-Dimethylamino-pyridine-3-yl)-8-azabicyclo[3.2.1]octane-8-carboxylic acid *tert*-butyl ester (13)

Triethylamine (0.86 ml, 6.17 mmol, 1.45 equiv) was added to a solution of **12** (0.95 g, 4.25 mmol) in THF (140 ml). After addition of a solution of di-*tert*-butyldicarbonate (1.35 g, 6.18 mmol, 1.45 equiv) in THF (10.5 ml), the reaction mixture was stirred for 4 h at RT. The solvent was removed in vacuo and the crude product was purified by column chromatography (ethyl acetate/hexane = 1:2). **13** (1.34 g, 95%) was obtained as white solid. ^{1}H NMR ($CDCl_3$, 500 MHz) two rotameric forms (RotA/RotB) result in a doubling of some signals: δ = 7.94–8.02 (m, 1H, RotA, 1H, RotB), 7.29–7.38 (m, 1H, RotA, 1H, 25 RotB), 6.47 (d, J = 8.8 Hz, 1H, RotA, 1H, RotB), 4.41 (bd, J = 7.1 Hz, 1H, RotA), 4.27 (bd, J = 7.0 Hz, 1H, RotB), 4.08 (bs, 1H, RotB), 3.96 (bs, 1H, RotA), 3.00 (m, 1H, RotA, 1H RotB), 3.05 (s, 6H, RotA), 3.04 (s, 6H, RotB), 2.15–2.26 (m, 1H, RotB), 2.19 (dd, J = 12.6, 9.5 Hz, 1H, RotA), 1.40–1.98 (m, 7H, RotA, 7H, RotB), 1.50 (s, 9H, RotA), 1.45 (s, 9H, RotB).

4.1.9. (−)-(1*R*,5*S*,6*S*)-5-(8-*tert*-Butoxycarbonyl-8-aza-bicyclo[3.2.1]oct-6-yl)-*N*,*N*,*N*-trimethylpyridine-2-aminium iodide ((−)-3)

Methyl iodide (25.1 ml, 404 mmol, 100 equiv) and potassium carbonate (20.8 g, 150.5 mmol, 37.5 equiv) were added successively to a solution of **13** (1.34 g, 4.04 mmol) in methanol (12.9 ml) under argon. The reaction flask was closed with a glass stopper and stirred under light exclusion for 5 d at rt. After this time the suspension was diluted with 130 ml dichloromethane and filtered. The filtrate was concentrated in vacuo to small volume, dissolved in 70 ml of ethyl acetate and quickly filtered over a syringe filter. The solvent was removed in vacuo. The residue was suspended in 100 ml of diethyl ether and intensively stirred for 1 h. The precipitate was isolated by suction filtration and washed three times with diethyl ether. The crude product was suspended in 50 ml of diethyl ether and 10 ml of dichloromethane. After stirring for 1 h at RT the precipitate was isolated by suction filtration and washed three times with diethyl ether. (−)-**3** (1.34 g, 70%) was obtained as white solid. ^{1}H NMR ($CDCl_3$, 500 MHz) two rotameric forms (RotA/RotB) result in a doubling of some signals: δ = 8.37 (d, J = 2.1 Hz, 1H, RotA, 1H, RotB), 8.29 (d, J = 8.0 Hz, 1H, RotB), 8.28 (d, J = 8.4 Hz, 1H, RotA), 7.92 (dd, J = 8.6, 1.9 Hz, 1H, RotA, 1H, RotB), 4.45 (bd, J = 7.0 Hz, 1H, RotB), 4.35 (bd, J = 6.9 Hz, 1H, RotA), 4.10 (bs, 1H, RotA), 4.06 (bs, 1H, RotB), 3.97 (s, 9H, RotB), 3.95 (s, 9H, RotA), 3.27–3.34 (m, 25 1H, RotB), 3.30 (dd, J = 9.1, 4.6 Hz, 1H, RotA), 2.28–2.38 (m, 1H, RotA, 1H, RotB), 1.98–2.08 (m, 1H, RotA), 1.41–1.97 (m, 6H, RotA, 7H, RotB), 1.50 (s, 9H, RotA), 1.48 (s, 9 H, RotB). ^{13}C NMR ($CDCl_3$, 126 MHz) two rotameric forms result in a doubling of signals: δ = 154.64, 153.16, 152.97, 146.94, 146.87, 146.20, 145.99, 139.04, 138.93, 115.25, 115.26, 79.72, 79.68, 61.46, 60.96, 55.67, 55.64, 55.06, 54.38, 44.29, 43.48, 38.75, 38.51, 30.41, 29.96, 29.58, 29.12, 28.41, 28.38, 16.76. $[\alpha]_D^{20}$ ($CHCl_3$, c = 5 mg/ml) = −47.4°. Elemental analysis –calculated: C 50.74 H 6.81 N 8.88 I 26.81 found: C 49.88 H 6.65 N 8.68 I 26.79.

4.1.10. (+)-(1*S*,5*R*,6*R*)-5-(8-*tert*-Butoxycarbonyl-8-aza-bicyclo[3.2.1]oct-6-yl)-*N*,*N*,*N*-trimethylpyridine-2-aminium iodide ((+)-3)

(+)-**3** was synthesized from (+)-**1**. All synthetic procedures and analytical data except optical rotation are identical with those reported for the synthesis of (−)-**3**. $[\alpha]_D^{20}$ ($CHCl_3$, c = 5 mg/ml) = +47.4°.

4.1.11. (−)-(1*R*,5*S*,6*S*)-6-(6-[^{18}F]Fluoro-pyridine-3-yl)-8-aza-bicyclo[3.2.1]octane ((−)-[^{18}F]flubatine, (−)-[^{18}F]1) and (+)-(1*S*,5*R*,6*R*)-6-(6-[^{18}F]fluoro-pyridine-3-yl)-8-aza-bicyclo[3.2.1]octane ((+)-[^{18}F]flubatine, (+)-[^{18}F]1)

[^{18}F]fluoride, produced with an IBA 18/9 cyclotron, was transferred into the reaction vial containing K_{222} in MeCN and aqueous K_2CO_3 solution. The mixture was azeotropically dried by repeated addition of anhydrous MeCN under reduced pressure in Argon atmosphere at 105 °C, for conversion of [^{18}F]F^- to the reactive K[^{18}F]F–K_{222}-carbonate complex. Typically, we used 11.2 mg (29.7 μmol) K_{222} and 1.78 mg (12.9 μmol) K_2CO_3. To the anhydrous K[^{18}F]F–K_{222}-carbonate complex, 0.75 ± 0.25 mg of the precursor (−)-**3** in 1.0 ml MeCN was added and reacted at 82 °C for 20 min. The labeling efficiency was 80–95% (n = 40), as monitored by radio-TLC. The crude product was diluted with 50 ml water, passed

through a Sep-Pak C18 cartridge and eluted with 1.0 ml 1% HOAc in MeCN in portions, typically resulting in a total eluted volume of 1.0 ml. Complete deprotection was obtained by adding 1 ml 1 M HCl to the eluates and warming at 90 °C for 6–8 min. After cooling, neutralization with 1 M NaOH, and dilution with water to a total volume of 4 ml, the mixture was applied to semi-preparative HPLC under isocratic conditions (column: Multospher 120 RP18 AQ 150 × 10 mm, 5 μm p.s.; eluent: 25% MeCN + 20 mM NH_4OAc, flow rate 0.75–1 ml/min). (−)-[^{18}F]**1** eluted at ~25 min. Combined separated fractions of (−)-[^{18}F]**1** (t_R ~20–25 min) were diluted with 20 ml water, adsorbed on one (or two) Sep-Pak C18 Plus cartridges and desorbed with 1% diethylamine in MeCN in small portions, resulting in an overall eluate volume of ~1.5 ml. The solvent was completely evaporated at 60 °C and the purified radiotracer was re-dissolved in sterile saline for animal experiments. The final product was analyzed by HPLC and TLC, indicating radiochemical yield of 55–65%, radiochemical purity of >99.5%, and specific activity of ⩾350 GBq/μmol with good reproducibility (n = 25), within a total synthesis time of about two hours. All radiochemical steps were routinely monitored by radio-HPLC and radio-TLC. TLC retention values R_f for MTBE/Et_3N 92:8 (v/v) were: (−)-[^{18}F]**14** = 0.83, (−)-[^{18}F]**1** = 0.27; and for chloroform/*iso*-propanol/NH_3 9.5:0.5:0,1 (v/v/v) were: (−)-[^{18}F]**14** = 0.73 and (−)-[^{18}F]**1** = 0.25. The analytical HPLC provided the following retention times: (−)-[^{18}F]**14** t_R ~38 min, (−)-[^{18}F]**1** t_R ~22 min (+)-[^{18}F]**1** was synthesized in an analogous way from (+)-**3**.

4.2. Receptor selectivity

The affinity of compounds (−)-**1** and (+)-**1** towards a variety of target proteins was investigated by radioligand displacement studies performed by Eurofins Panlabs Taiwan, Ltd (Pharmacology Laboratories, Taipei, Taiwan R.O.C.). K_i values were determined for binding towards human α4β2 nAChR, human α1 nAChR, rat α4β2 nAChR, and rat α7 nAChR. At 10 μM concentration, the inhibitory potential of compounds (−)-**1** and (+)-**1** was tested for adenosine receptors A_1, A_{2A}, and A_3, adrenergic receptors α_1, α_2 and β, calcium channel L-type, calcium channel N-type, dopamine receptors D_1, D_{2L}, D_{2S}, D_3, $D_{4,2}$, $D_{4,4}$, $D_{4,7}$, and D_5, $GABA_A$ receptors of the cerebellum and of the hippocampus, histamine receptors H_1, H_2, H_3, and H_4, muscarinic receptors M_1, M_2, M_3, M_4, and M_5, opiate receptors (non-selectively), potassium channels K_{ATP} and hERG, serotonin receptors 5-HT_{1A}, 5-HT_{2A}, 5-HT_{2B}, 5-HT_{2C}, and 5-HT_3, adenosine transporter, the monoamine transporters DAT, NET, and SERT, as well as cyclooxygenases COX-1 and COX-2.

4.3. Toxicity studies

A GLP conform extended single dose toxicity study regarding (−)-**1** was performed by Harlan Laboratories Ltd. The compound was administered once, intravenously to WI(Han) rats at a dosage of 6.2, 24.8, and 124 μg/kg, with six males and six females in each dosage group killed at days 2 and 14. A further GLP conform extended single dose toxicity study regarding (+)-**1** was performed by BSL BIOSERVICE Scientific Laboratories GmbH. The compound was administered once, intravenously to WI(Han) rats at a dosage of 1.55, 12.4 and 31 μg/kg, with thirty males and thirty females in each dosage group killed at days 2 and 14.

4.4. Autoradiography (pig)

Animal experiments were performed under procedures approved by the respective State Animal Care and Use Committee and conducted in accordance with the German Law for the Protection of Animals. Juvenile female pigs (mixed German domestic breed, 36–40 kg) were anesthetized (midazolam, 1 mg/kg, im, + ketamine 12 mg/kg, im) and killed by intravenous infusion of 10 ml saturated potassium chloride. Brains were removed rapidly, frozen in isopentane/dry ice at −35 °C, and stored at −50 °C until cryostat slices were prepared. The autoradiographic analyses were performed using sagittal 20 μm brain cryostat sections (MICROM, Germany) mounted on glass slides as follows: The sections were thawed at room temperature, pre-incubated with incubation buffer (50 mM TRIS–HCl, pH 7.4, 120 mM NaCl, 5 mM KCl, 2.5 mM $CaCl_2$, 1 mM $MgCl_2$) for 10 min at room temperature followed by an incubation with serial dilutions (1 pM to 15 nM) of the respective radiotracers (−)-[^{18}F]**1** and (+)-[^{18}F]**1** for 90 min at room temperature. Nonspecific binding was determined in the presence of 300 μM nicotine. Afterwards, the sections were washed twice with 50 mM TRIS–HCl, pH 7.4, for 2 min at 4 °C, rinsed with ice-cold ultra pure water, air dried, and exposed to ^{18}F-sensitive imaging plates (Fuji Film, Japan). The phosphoimaging plates were read by laser scanning (BAS-1800 II; Fuji Film, Japan) and quantitative analysis of the scan data was performed by computer assisted micro densitometry (Aida 2.31; Raytest, Germany). Regions of interest (ROIs) were drawn and subsequently confirmed by Nissl staining. The optical density obtained for each ROI was obtained primarily as photostimulated luminescence per area (PSL/mm^2), corrected for background and converted to fmol/mg protein. The binding parameters K_D and B_{max} were estimated by nonlinear regression analysis.

Acknowledgments

This work was supported by a Grant of the German Federal Ministry of Education and Research (Grant Code: 01EZ0821), which is gratefully acknowledged. We wish to thank the staff of the cyclotron facility at the Department of Nuclear Medicine, University of Leipzig, and Karsten Franke from our own IBA 18/9 Cyclotron Unit for providing [^{18}F]fluoride. We are grateful to Antje Berthold, Andreas Clausnitzer, Tina Spalholz and Juliane Schaller for their technical assistance. We thank Anne Jäger and Dirk Meyer from the Technical University of Dresden who conducted the X-ray diffraction studies.

Supplementary data

Supplementary data associated with this article can be found, in the online version, at http://dx.doi.org/10.1016/j.bmc.2013.12.011.

References and notes

1. Joshi, A. D.; Pontecorvo, M. J.; Clark, C. M.; Carpenter, A. P.; Jennings, D. L.; Sadowsky, C. H.; Adler, L. P.; Kovnat, K. D.; Seibyl, J. P.; Arora, A.; Saha, K.; Burns, J. D.; Lowrey, M. J.; Mintun, M. A.; Skovronsky, D. M. *J. Nucl. Med.* **2012**, *53*, 378.
2. Herholz, K.; Ebmeier, K. *Lancet Neurol.* **2011**, *10*, 667.
3. Kurz, A.; Perneczky, R. *J. Alzheimers Dis.* **2011**, *24*, 61.
4. Graef, S.; Schönknecht, P.; Sabri, O.; Hegerl, U. *Psychopharmacology (Berlin, Ger.)* **2011**, *215*, 205.
5. Lindstrom, J.; Anand, R.; Peng, X.; Gerzanich, V.; Wang, F.; Li, Y. *Ann. N.Y. Acad. Sci.* **1995**, *757*, 100.
6. Baddick, C. G.; Marks, M. J. *Biochem. Pharmacol.* **2011**, *82*, 828.
7. Perry, E. K.; Martin-Ruiz, C. M.; Court, J. A. *Alcohol* **2001**, *24*, 63.
8. Perry, E.; Martin-Ruiz, C.; Lee, M.; Griffiths, M.; Johnson, M.; Piggott, M.; Haroutunian, V.; Buxbaum, J. D.; Nasland, J.; Davis, K.; Gotti, C.; Clementi, F.; Tzartos, S.; Cohen, O.; Soreq, H.; Jaros, E.; Perry, R.; Ballard, C.; McKeith, I.; Court, J. *Eur. J. Pharmacol.* **2000**, *393*, 215.
9. Kadir, A.; Almkvist, O.; Wall, A.; Langström, B.; Nordberg, A. *Psychopharmacology (Berlin, Ger.)* **2006**, *188*, 509.
10. O'Brien, J. T.; Colloby, S. J.; Pakrasi, S.; Perry, E. K.; Pimlott, S. L.; Wyper, D. J.; McKeith, I. G.; Williams, E. D. *J. Neurol. Neurosurg. Psychiatry* **2007**, *78*, 356.
11. Kendziorra, K.; Wolf, H.; Meyer, P. M.; Barthel, H.; Hesse, S.; Becker, G. A.; Luthardt, J.; Schildan, A.; Patt, M.; Sorger, D.; Seese, A.; Gertz, H. J.; Sabri, O. *Eur. J. Nucl. Med. Mol. Imaging* **2011**, *38*, 515.
12. Valette, H.; Dolle, F.; Saba, W.; Roger, G.; Hinnen, F.; Coulon, C.; Ottaviani, M.; Syrota, A.; Bottlaender, M. *Synapse* **2007**, *61*, 764.
13. Kuwabara, H.; Wong, D. F.; Gao, Y.; Valentine, H.; Holt, D. P.; Ravert, H. T.; Dannals, R. F.; Horti, A. G. *J. Nucl. Med.* **2012**, *53*, 121.

14. Deuther-Conrad, W.; Patt, J. T.; Feuerbach, D.; Wegner, F.; Brust, P.; Steinbach, J. *Farmaco* **2004**, *59*, 785.
15. Deuther-Conrad, W.; Patt, J. T.; Lockman, P. R.; Allen, D. D.; Patt, M.; Schildan, A.; Ganapathy, V.; Steinbach, J.; Sabri, O.; Brust, P. *Eur. Neuropsychopharmacol.* **2008**, *18*, 222.
16. Brust, P.; Patt, J. T.; Deuther-Conrad, W.; Becker, G.; Patt, M.; Schildan, A.; Sorger, D.; Kendziorra, K.; Meyer, P.; Steinbach, J.; Sabri, O. *Synapse* **2008**, *62*, 205.
17. Hockley, B. G.; Stewart, M. N.; Sherman, P.; Quesada, C.; Kilbourn, M. R.; Albin, R. L.; Scott, P. J. H. *J. Labelled Compd. Radiopharm.* **2013**, *56*, 595.
18. Patt, J. T.; Deuther-Conrad, W.; Wohlfahrt, K.; Feuerbach, D.; Brust, P.; Steinbach, J. *J. Labelled Compd. Radiopharm.* **2003**, *46*, S168.
19. Bai, D.; Xu, R.; Chu, G.; Zhu, X. *J. Org. Chem.* **1996**, *61*, 4600.
20. Patt, J. T.; Deuther-Conrad, W.; Brust, P. *[^{18}F]Norchloro-Fluoro-Homoepibatidine: Synthesis, Radiosynthesis, Evaluation In Vitro and Comparison of the Biodistribution with 2-[^{18}F]Fluoro-A-85380 in Mice*; Institute of Interdisciplinary Isotope Research: Leipzig, 2003. Annual Report.
21. Kim, H.; Hoffmann, H. M. R. *Eur. J. Org. Chem.* **2000**, 2195.
22. Drew, M. G. B.; George, A. V.; Isaacs, N. S. *J. Chem. Soc., Perkin Trans. 1* **1985**, 1277.
23. Mann, J.; de Almeida Barbosa, L.-C. *J. Chem. Soc., Perkin Trans. 1* **1992**, 787.
24. Cramer, N.; Laschat, S.; Baro, A.; Frey, W. *Synlett* **2003**, 2175.
25. Hodgson, D. M.; Paruch, E. *Tetrahedron* **2004**, *60*, 5158.
26. Larock, R. C.; Johnson, P. L. *J. Chem. Soc., Chem. Commun.* **1989**, 1368.
27. Arcadi, A.; Marinelli, F.; Bernocchi, E.; Cacchi, S.; Ortar, G. *J. Organomet. Chem.* **1989**, *368*, 249.
28. Wu, X.-Y.; Xu, H.-D.; Zhou, Q.-L.; Chan, A. S. C. *Tetrahedron: Asymmetry* **2000**, *11*, 1255.
29. Wu, X.-Y.; Xu, H.-D.; Tang, F.-Y.; Zhou, Q.-L. *Tetrahedron: Asymmetry* **2001**, *12*, 2565.
30. Namyslo, J. C.; Kaufmann, D. E. *Synlett* **1999**, 804.
31. Clayton, S. C.; Regan, A. C. *Tetrahedron Lett.* **1993**, *34*, 7493.
32. Herrmann, W. A.; Broßmer, C.; Öfele, K.; Reisinger, C.-P.; Priermeier, T.; Beller, M.; Fischer, H. *Angew. Chem., Int. Ed.* **1995**, *34*, 1844.
33. Kim, Y. H.; Won, D. Y.; Oh, C. Y.; Lee, K. Y.; Jeong, J. H.; Jung, Y. H.; Ham, W. H. *Arch. Pharmacol. Res.* **1999**, *22*, 435.
34. Moreno-Vargas, A. J.; Vogel, P. *Tetrahedron: Asymmetry* **2003**, *14*, 3173.
35. Liang, F.; Navarro, H. A.; Abraham, P.; Kotian, P.; Ding, Y.-S.; Fowler, J.; Volkow, N.; Kuhar, M. J.; Carroll, F. I. *J. Med. Chem.* **1997**, *40*, 2293.
36. Fischer, S.; Hiller, A.; Smits, R.; Hoepping, A.; Funke, U.; Wenzel, B.; Cumming, P.; Sabri, O.; Steinbach, J.; Brust, P. *Appl. Radiat. Isot.* **2013**, *74*, 128.
37. Patt, M.; Schildan, A.; Habermann, B.; Fischer, S.; Hiller, A.; Deuther-Conrad, W.; Wilke, S.; Smits, R.; Hoepping, A.; Wagenknecht, G.; Steinbach, J.; Brust, P.; Sabri, O. *Appl. Radiat. Isot.* **2013**, *80*, 7.
38. Deuther-Conrad, W.; Wevers, A.; Becker, G.; Schildan, A.; Patt, M.; Sabri, O.; Steinbach, J.; Brust, P. *Synapse* **2006**, *59*, 201.
39. Gatley, S. J.; Ding, Y. S.; Brady, D.; Gifford, A. N.; Dewey, S. L.; Carroll, F. I.; Fowler, J. S.; Volkow, N. D. *Nucl. Med. Biol.* **1998**, *25*, 449.
40. Han, Z. Y.; Zoli, M.; Cardona, A.; Bourgeois, J. P.; Changeux, J. P.; Le Novere, N. *J. Comp. Neurol.* **2003**, *461*, 49.
41. Sihver, W.; Gillberg, P. G.; Nordberg, A. *Neuroscience* **1998**, *85*, 1121.
42. Moser, N.; Mechawar, N.; Jones, I.; Gochberg-Sarver, A.; Orr-Urtreger, A.; Plomann, M.; Salas, R.; Molles, B.; Marubio, L.; Roth, U.; Maskos, U.; Winzer-Serhan, U.; Bourgeois, J. P.; Le Sourd, A. M.; De Biasi, M.; Schröder, H.; Lindstrom, J.; Maelicke, A.; Changeux, J. P.; Wevers, A. *J. Neurochem.* **2007**, *102*, 479.
43. Gallezot, J. D.; Bottlaender, M. A.; Delforge, J.; Valette, H.; Saba, W.; Dolle, F.; Coulon, C. M.; Ottaviani, M. P.; Hinnen, F.; Syrota, A.; Gregoire, M. C. *J. Cereb. Blood Flow Metab.* **2008**, *28*, 172.
44. Pimlott, S. L.; Piggott, M.; Owens, J.; Greally, E.; Court, J. A.; Jaros, E.; Perry, R. H.; Perry, E. K.; Wyper, D. *Neuropsychopharmacology* **2004**, *29*, 108.